AGU PUBLICATIONS

Geophysical Research Letters

RESEARCH LETTER
10.1002/2017GL073124

Key Points:
- A novel way to quantify the relative contributions of mesoscale extratropical cyclone features is introduced
- Larger-scale features are most commonly associated with the top 1% of UK surface gusts but smaller-scale features generate the most extreme 0.1% of winds
- Sting jets and convective lines account for two thirds of severe surface gusts in the UK

Supporting Information:
- Supporting Information S1

Correspondence to:
N. Earl,
nearl@unimelb.edu.au

Citation:
Earl, N., S. Dorling, M. Starks, and R. Finch (2017), Subsynoptic-scale features associated with extreme surface gusts in UK extratropical cyclone events, *Geophys. Res. Lett.*, *44*, 3932–3940, doi:10.1002/2017GL073124.

Received 17 FEB 2017
Accepted 12 APR 2017
Accepted article online 18 APR 2017
Published online 30 APR 2017

Subsynoptic-scale features associated with extreme surface gusts in UK extratropical cyclone events

N. Earl[1,2], S. Dorling[1], M. Starks[1], and R. Finch[1]

[1]School of Environmental Sciences, University of East Anglia, Norfolk, UK, [2]School of Earth Sciences, University of Melbourne, Melbourne, Victoria, Australia

Abstract Numerous studies have addressed the mesoscale features within extratropical cyclones (ETCs) that are responsible for the most destructive winds, though few have utilized surface observation data, and most are based on case studies. By using a 39-station UK surface observation network, coupled with in-depth analysis of the causes of extreme gusts during the period 2008–2014, we show that larger-scale features (warm and cold conveyer belts) are most commonly associated with the top 1% of UK gusts but smaller-scale features generate the most extreme winds. The cold conveyor belt is far more destructive when joining the momentum of the ETC, rather than earlier in its trajectory, ahead of the approaching warm front. Sting jets and convective lines account for two thirds of severe surface gusts in the UK.

1. Introduction

European extratropical cyclones (ETCs) are the most economically significant weather hazard when averaging insured losses over multiple years, as exemplified by the "16 October 1987 Storm" in the UK [*Woodroffe*, 1988; *Browning*, 2004], by Windstorm Gudrun of 2005 [*Baker*, 2009], and by Windstorm Kyrill of 2007 [*Brönnimann et al.*, 2012]. From 1970 to 2015, 32 of the 40 most expensive worldwide insured loss events were weather related, nine of which were located in Europe and associated with ETCs, generating hurricane force surface winds and widespread flooding [*Swiss Re*, 2016]. This paper explores the mesoscale features within ETCs which are associated with observed extreme surface winds.

There has been much research addressing the synoptic-scale structure of ETCs since the development of the Norwegian cyclogenesis model [*Bjerknes and Solberg*, 1922]. It was the first conceptualized ETC life cycle model, locating cyclogenesis along the polar front and dividing the cycle into stages of the typical life of a low-pressure system in the extratropics [*Parton et al.*, 2010]. Development of the ETC life cycle conceptual model evolved into the conveyer belt paradigm [*Browning*, 1990] (Figure 1b) and the development of the *Shapiro and Keyser* [1990] cyclone model (Figure 1a). In addition, *Schultz and Vaughan* [2011] provided a modified view of the occlusion front paradigm within the Norwegian cyclogenesis model suggesting that viewing the occlusion process as wrap-up rather than catch-up resolves anomalies within the conceptual model.

Browning [2004] identified one of the causes of the most extreme surface winds to be associated with a mesoscale feature at the tip of the cloud head as the "sting at the end of the tail" (shortened to sting jet; SJ) (Table 1 and Figure 1b). This proved to be the case for the 16 October 1987 storm [*Clark et al.*, 2005], for Windstorm Jeanette in October 2002 [*Parton et al.*, 2009], and Christian in October 2013 [*Browning et al.*, 2015], amongst others. However *Baker* [2009] found that the strongest surface winds during Windstorm Gudrun of January 2005 were associated with the cold conveyer belt (CCB) as it wrapped around the low-pressure center and acted in the same direction as the motion of the cyclone. *Hewson and Neu* [2015] broke down storms into distinct features, SJ, CCB, and warm-conveyor belt (WCB) explaining where the extreme surface winds occur in relation to a typical ETC track. The WCB starts at low levels before rising over the warm front above the cold air below. It is most likely to affect the surface in the warm sector, just ahead of the cold front, rather than nearer the warm front where it has been forced upward (Figure 1b). The WCB produces the largest footprint of strong surface winds, though these are not as severe as the CCB or SJ [*Hewson and Neu*, 2015]. *Clark* [2013] developed a climatology of convective lines (CL; comprising mainly narrow cold frontal rainbands and postfrontal quasilinear convective systems (QLCSs)). These lines of organized and strong convection occur mainly along cold frontal boundaries in the UK, though a few occur in association with occluded fronts. Prefrontal QLCSs were not included in *Clark*'s [2013] climatology. This CL climatology was not constructed with surface wind gusts in mind; however, CLs, especially QLCSs, are well known for

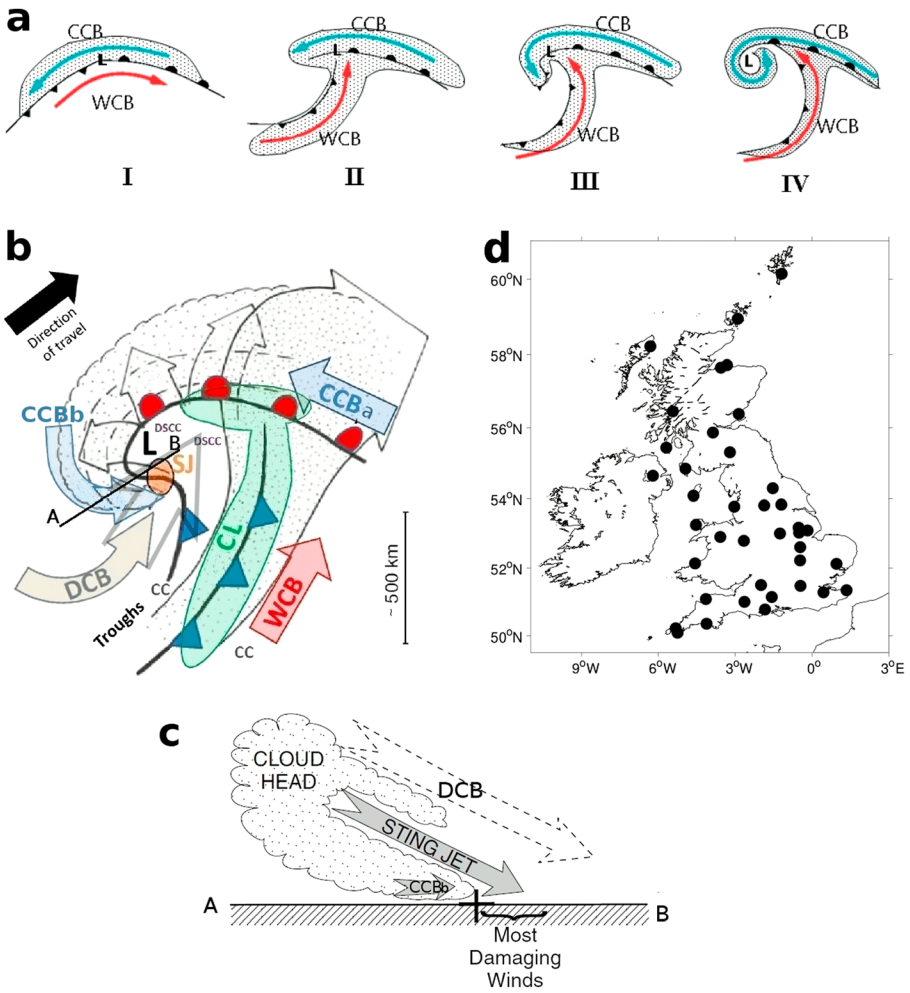

Figure 1. (a) Shapiro-Keyser conceptual model of the life cycle of an extratropical cyclone: (I) open wave, (II) frontal fracture, (III) bent-back front and frontal T-bone, and (IV) mature, frontal seclusion. The cold and warm conveyor belts (CCB and WCB, respectively) are marked along with the low-pressure center (L) and the cloud signature (stippled areas) (adapted from *Baker* [2009]). (b) Conceptual model of subsynoptic-scale features within an extratropical cyclone, during transition from stage III to stage IV (adapted from *Browning* [2004]). See Tables 1 and S1 for an explanation of WCB, CCBa, CCBb, DCB, SJ (orange shading), CC, CL (green shading), and DSCC. (c) Vertical cross section through the A–B line (in Figure 1b), displaying the relative positions of the conveyor belts seen during sting jets and the region of cloud (adapted from *Clark et al.* [2005]). (d) Locations of the 39 UK wind monitoring sites used in this study.

producing strong winds, including intense downburst winds, a rear inflow jet [*Weisman*, 2001], and low-level mesovortices, all of which produce damaging winds [*Davis et al*., 2004; *Wheatley et al*., 2006]. The rear inflow jet and mesovortices usually travel perpendicular to the orientation of the line, as distinct from the winds within the parallel-flowing WCB, which is found ahead of many narrow cold frontal rainbands in ETCs [*Browning*, 2004]. QLCSs are particularly common in the USA and are sometimes known as squall lines. QLCSs that present a strongly bulging structure are referred to as bow echoes [*Weisman*, 2001]. These systems have also been reported in Europe [*Gatzen et al*., 2011].

Table 1 summarizes the characteristics of the conveyor belts and other ETC subsynoptic-scale features, and Figure 1b displays the respective locations of these features within a Shapiro-Keyser conceptual ETC, where the highest surface impacts are likely during transition from stage III to stage IV of the Shapiro-Keyser conceptual model of the life cycle. The A-B cross section in Figure 1c shows the relative vertical positions of the SJ, CCBb, and the dry conveyor belt (DCB) in ETCs which possess a well-developed SJ that reaches the surface.

Not all ETCs will follow the Shapiro-Keyser conceptual model life cycle, depending on whether the ETC is embedded in diffluent or confluent large-scale flow in the upper levels and, if the former, will tend to

Table 1. Allocations of Features[a]

Feature	Description
Cold conveyor belt (CCBa)	DMGS occurs ahead (usually east) of the surface warm front, identified by the foregoing precipitation and cloud signatures in the satellite and radar images. The gust is often orientated parallel to the front travelling toward the low pressure center.
Cold conveyor belt (CCBb)	DMGS is located equatorward or west of the low-pressure center, usually directly beneath (but not at the tip of) the cloud and precipitation signature. Pressure charts indicate high-pressure gradients in this part of the ETC. The gust is usually orientated equatorward or in the direction of ETC travel, occurring in stage IV of the Shapiro-Keyser life cycle model.
Warm conveyor belt (WCB)	This usually broad region of poleward flowing air often affects the surface relatively early in the life cycle (stages II–III). Located between, but clearly separate from, the two primary fronts and often flows parallel to the cold front (rather than perpendicular as for CLs).
Dry conveyor belt (DCB)	The dry slot is in a region of clearing skies behind the cold front, clearly distinct from the main precipitation and cloud signatures in the radar and satellite images, with no radar echo or visible cloud. DMGS occurs in this region, with no sign of cellular convection apparent.
Convective lines (CL)	Lines of organized and strong convection, very clear signal in the radar images. DMGS is usually travelling perpendicular to the orientation of the front line (distinct from the WCB). To be classified as a CL, the feature has to meet *Clark*'s [2013] threshold criteria (see Table S1)
Sting jet (SJ)	DMGS at the tip of the cloud head hook often clearly visible in the radar and satellite images. Only identified in stages II and III of the Shapiro-Keyser life cycle model and replaced by the CCBb in stage IV. ETC must be rapidly deepening ($\geq$ one Bergeron), there must be clear evidence of cloud banding and DMGS located within 100 km of the cloud hook tip.
Dry slot cellular convection (DSCC)	Cellular convection that occurs within the dry slot producing heavy showers visible on the radar images at the site location during the time of DMGS.
Cellular convection (CC)	Area of unorganized convection outside of the dry intrusion producing heavy showers visible on the radar images at the site location during the time of DMGS.
Pseudo-convective lines (pseudo-CL)	As with CLs but do not reach the status of CL as defined by *Clark* [2013], though do possess the same distinct characteristics. Also included are lines visible on the radar images, which were classified as CLs earlier or later in the day but which were not so classified at the time of DMGS.

[a]Description of allocating DMGSs to specific ETC features.

follow a life cycle more akin to the Norwegian life cycle model as explored by *Schultz et al.* [1998]. Also, many ETCs will not contain all of these subsynoptic-scale features, some, for example, exhibit insufficient deepening rate ($<$ 1 Bergeron), a major factor in producing SJs [*Browning*, 2004]. Furthermore, subsynoptic-scale features may be present in many ETCs, such as a SJ or DCB, but their presence may not result in an extreme gust being recorded at the surface. However, all features shown in Figure 1b have been observed to cause extreme surface wind speeds in some ETCs.

Most studies rely on tracking algorithms for intense ETC identification, often based on reanalysis resolution data [*Neu et al.*, 2013; *Hewson and Neu*, 2015]. Many mesoscale features are subgrid scale for these, so the intensity of surface winds is poorly represented. This paper introduces a novel way to quantify the relative contributions of mesoscale ETC features, based on surface wind observations. The approach used here is distinct from previous climatological studies, for example, *Parton et al.* [2010], *Clark* [2013], and *Martínez-Alvarado et al.* [2012], who used midtropospheric observations, radar imagery, and ERA-Interim data, respectively, without specific reference to observed wind speeds at the surface. It is also complementary to *Hewson and Neu* [2015] in their IMILAST project ("Intercomparison of MId-LAtitude STorm diagnostics," first described in *Neu et al.* [2013]) based on storm track algorithms.

2. Data and Methods

2.1. Observational Network and Extreme Wind Identification

The events used in this study are identified using the UK observational daily maximum gust speed (DMGS) database, introduced by *Hewston and Dorling* [2011] and also analyzed in *Earl et al.* [2013]. This covers the period 1980–2014, consisting of 39 UK wind monitoring sites (Figure 1d). This research was completed in conjunction with an associated forecast verification study [*Earl*, 2013], the data for which began in 2008; therefore, the work presented here covers the period 2008–2014. The DMGSs are ranked in order of intensity for each of the 39 observational network sites, and the top 1% (128 strongest DMGSs plus those tied for rank 128) and 0.1% (13 strongest DMGSs; hereafter, 1%DMGS and 0.1%DMGS) during the whole 1980–2014 period are highlighted at each site (placing the 2008–2014 period into a longer context). The absolute wind

speeds vary greatly throughout the network, with the 99.9th percentile at Lerwick, for example, being 81 kt, whereas at Heathrow, the equivalent percentile was just 55 kt. During the development of a windstorm loss model, *Hewston* [2008] found that it was only the top 2% of local DMGSs that resulted in damage to insured property. Concentrating here on the 1%DMGSs and 0.1%DMGSs therefore places specific emphasis on the most damaging winds. Each 1%DMGS and 0.1%DMGS is then associated with a corresponding ETC (no other causes were evident during the period 2008–2014). ETC names, as allocated by the Free University of Berlin, are used for the identified ETCs. Only ETC events which are associated with more than one 1%DMGS, be it at more than one station or a single station on successive days, are included in the study, to minimize the possible impact of erroneous measurement data.

2.2. Feature Allocation

Allocation of each of the 1%DMGS (or 0.1%DMGS) to associated subsynoptic-scale features (Figure 1b) is undertaken manually, using surface pressure charts (courtesy of UK Met Office), 15 min rainfall radar images (from the UK Met Office NIMROD system), and satellite imagery (courtesy of the University of Dundee Satellite Receiving Station), along with the data from the surface observation network (accurate to 1 min). Once the DMGS has been identified, the most temporally applicable 6-hourly surface pressure charts are used along with the applicable satellite images to identify the main features of the ETC and establish the stage of Shapiro-Keyser life cycle. These are then compared with the radar images which are closest in time to the gust event for feature assignment (e.g., fronts, troughs, and low-pressure center). The high temporal resolution radar images are essential, providing the opportunity to accurately track the cyclone features through time, highlighted by the precipitation signature, until the time of the DMGS in question at the specific station. Table 1 provides a description of the mechanism allocation. When a 1% (0.1%) DMGS is not judged to be associated with any subsynoptic-scale feature, it is identified as being "unclassifiable." Once all of the subsynoptic-scale features cause for all 1% (0.1%) DMGS have been categorized, they are then assembled as a 2008–2014 climatology of 1% (0.1%) DMGS gust-causing features. (See Figure S1 and Text S1 in the supporting information for three examples of 0.1%DMGS allocation).

We acknowledge that some extreme gusts may be missed by our method due to the spatially irregular nature of the observation network (Figure 1d), especially the smaller-scale features such as SJs. Also, only including the DMGS (one per day per station) means omitting some extreme gusts seen on the same day often from a different mechanism.

3. Results

3.1. Interannual and Intraannual Variability of 1980–2014 Extreme DMGS

Results presented in *Earl et al.* [2013] showed that the years 2008–2010 saw a well-below-average frequency of high daily mean wind speeds compared to the early 1980s and early 1990s. Since then there has been a recovery. Therefore, before analyzing the 2008–2014 1%DMGS and 0.1%DMGS observations, we explore the full 1980–2014 DMGS surface station measurement database to highlight the 2008–2014 period's relative contribution to 1980–2014 extremes. This sets the 2008–2014 period in the context of the longer climatological record.

Figure 2a presents the 1980–2014 interannual distribution of 1%DMGS and 0.1%DMGS totals, providing an insight into the main periods of extreme storminess. There is a large interannual range for both percentiles, lowest in 2010 with just 19 occurrences of 1%DMGS (0.4% of the 35 year total) and no 0.1%DMGS. Similarly, low values occurred in 2001 and 2003. The highest values for both percentiles occurred during 1993 with 371 (7.1%) of 1%DMGSs and 77 (14%) of 0.1%DMGSs. The early 1980s and early 1990s stand out as periods of more frequent extreme wind speeds, the 2000s much less so, in accordance with other related mean wind speed studies in the literature for the UK and Europe as a whole [*Wang et al*., 2009; *Vautard et al*., 2010; *Earl et al*., 2013]. This is strongly linked to the phase of the North Atlantic Oscillation (NAO) [*Earl et al*., 2013] and ETC activity in the Atlantic [*Tilinina et al*., 2013]. A positive NAO means a stronger pressure gradient between the Icelandic low and Azores high, bringing more zonal conditions to the North Atlantic and consequently more windstorms to northern Europe. Since 2011, extreme wind speeds have increased toward longer-term average frequencies, but are still below average, in agreement with recent NAO variability [*Hanna et al*., 2015].

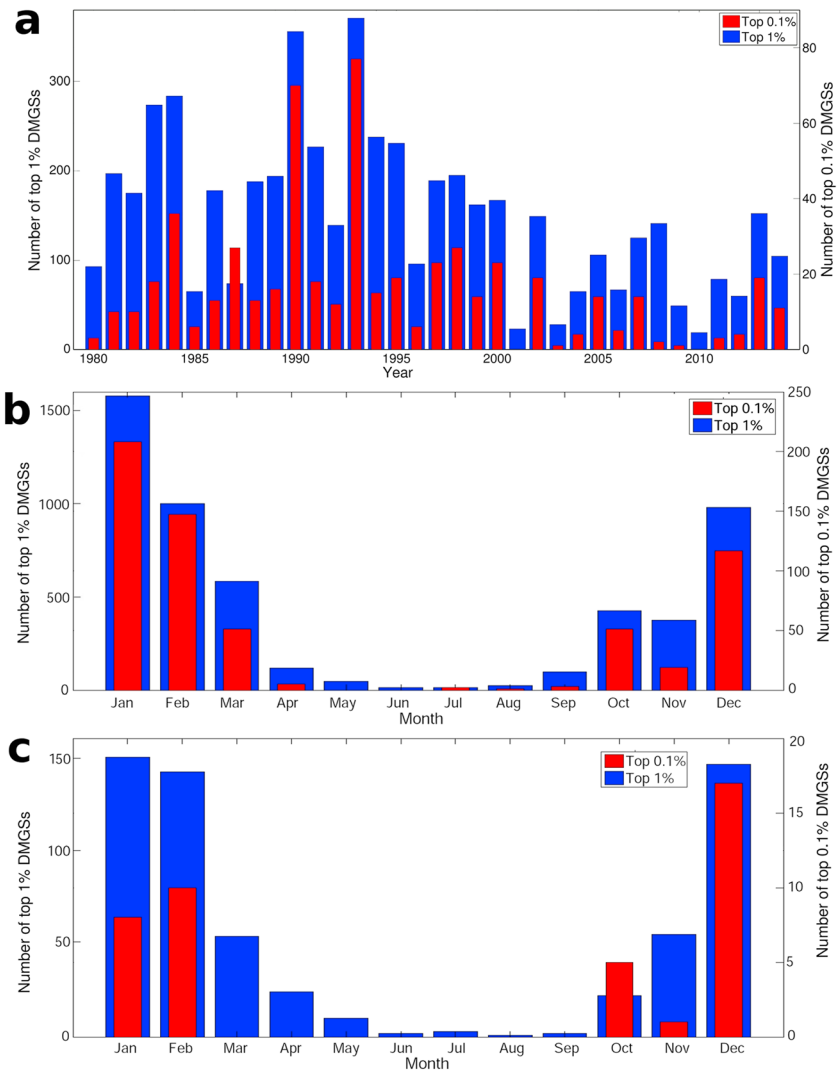

Figure 2. (a) The 1980–2014 interannual variability in the frequency of top 1% (1%DMGS) and 0.1% (0.1%DMGS) occurrences (totals: 5256 and 554, respectively) for all 39 stations. (b) The 1980–2014 monthly distribution of 1%DMGSs and 0.1%DMGSs. (c) The 2008–2014 monthly distribution of 1%DMGSs and 0.1%DMGSs. Note that top 0.1% DMGS total is more than 507 (39 sites times 13 (top 0.1% of 35 years)) due to DMGSs tied for rank 13 at some sites (same occurs with top 1%).

Generally 2008–2014 was a low-wind speed period; only 2013 recorded close to average (~150) top 1%DMGS frequency. The 0.1%DMGSs show even "leaner" storminess in this period, with an average of 8.2 occurrences per year, well below the annual average of 15.7 over the longer period. The unprecedented storminess of the early 1990s [*Wang et al*., 2009; *Earl et al*., 2013], highlighted by the strongest positive NAO index on record (1899–2014) [*Hanna et al*., 2015], can be seen to be largely due to exceptionally stormy years in 1990 and 1993, neighboring years being much closer to the 0.1%DMGS 35 year average. The years 2008 and 2013 accounted for twice the number of 1%DMGSs compared with the famous 1987, whereas the 1987 0.1% DMGSs outweigh those attributed to 2008 and 2013; there was no 2008–2014 storm of a comparable magnitude to the 16 October 1987 storm which, at the time, sets records for insured losses for a natural catastrophe [*Swiss Re*, 2016].

Figure 2b shows that winter months (December-January-February) in the 1980–2014 period account for 67.7% of 1%DMGS and 75.6% of 0.1%DMGS, January being the dominant contributor to both percentiles followed by February and then December; winter is the time of year when synoptic conditions best accommodate extreme ETCs to track across the UK due to the higher-pressure gradients across the region [*Wang*

et al., 2009]. The month of October, so influential in 1987, is less prominent, though does account for more DMGS extremes than November for both percentiles. The months from April to September rarely contribute to the highest DMGSs. January experienced 208 (37.5%) of the total 0.1%DMGSs, January 1993 the stormiest of all, accounting for 58, including the mid-January Braer Storm producing 23 0.1%DMGSs. On 25 January 1990, Windstorm Daria produced 22 0.1%DMGSs on a single day. Other prominent UK windstorms causing heavy insured losses and impacting the 0.1%DMGS climatology include Jeanette of late October 2002 (12 0.1%DMGS occurrences), Erwin in January 2005 (12), Windstorm Kyrill on 18 January 2007 (14), and Xaver on 5 December 2013 (7) (Table S2). With high-profile storms featuring so prominently in the extreme DMGS part of the observation database, additional confidence can be placed in its ability to accurately represent the UK's extreme wind regime.

Figure 2c shows that the 2008–2014 monthly distribution of the 1%DMGSs is also dominated by January-February-December. This period also continues the longer-term pattern of more 0.1%DMGSs during October than November, indicating that this 7 year period provides a good representation of the longer-term record, despite being a period of "leaner" storminess. With the relatively high number of October 0.1% DMGSs, along with no events between March and September, the impact of October events will be enhanced due to summer vegetation growth and trees often still being in leaf, a reason why the "16 October 1987 Storm" was so damaging [*Woodroffe*, 1988; *Browning*, 2004]. The reason behind this October spike is unclear; however, the analysis of "singularities" in the post–World War II era, chiefly by *Lamb* [1950], suggested that mid-November in the UK often includes an 11 day period of calm anticyclonic weather. Lamb analyzed the 1898–1947 temporal period, so there is no overlap with our study, and the singularities theory is controversial; however, this may provide a possible explanation for the relative lull in November extreme wind activity.

3.2. The 2008–2014 Storm Set Identification

Despite the relatively low windiness of the 2008–2014 period, there were 600 examples of 1%DMGSs and 41 0.1%DMGSs experienced at the 39 network sites, from which a number of individual windstorms may be identified. A total of 73 unique ETC events, shown in Table S2, each resulted in at least two occurrences of 1%DMGS.

Despite the lower overall frequency of strong wind events in this period, compared to the 1980–2014 average, there were many newsworthy storms which caused widespread damage and disruption across the UK including the aforementioned Xaver and Christian (the "St Jude's Day" windstorm 28 October 2013), the latter shown to have produced a SJ [*Browning et al*., 2015].

The damaging gusts associated with some ETCs can be felt over very small spatial scales and contain exceptionally strong winds, e.g., Christian (eight top 1%DMGSs, five of which were 0.1%DMGSs), compared to events which stand out on a more national scale, such as storm Emma (29 February 2008; 25 1%DMGSs but no 0.1%DMGSs). Two events which attracted much media coverage in Europe between 2008 and 2014 were Windstorms Klaus (January 2009) and Xynthia (March 2010), but the track of these left the UK unscathed in terms of 1%DMGSs at any of the network sites.

3.3. The 2008–2014 Climatology for Subsynoptic-Scale Feature Contributions to 1%DMGS

Subjectively classified features associated with all DMGSs, from each of the 73 ETC events, are summarized in Table 2.

Over the 2008–2014 period, the CCBb accounted for over 34% of all 1%DMGS, the WCB being the second most influential feature. These conveyor belts are widely known to regularly cause extreme surface winds within ETCs [e.g., *Browning*, 2004; *Hewson and Neu*, 2015], and the results are comparable, proportionally, to those of *Parton et al.* [2010] who focused on the midtroposphere. The CCBa only accounted for 5% of 1%DMGSs, highlighting that this part of the CCB feature is far less likely to be associated with extreme winds than the CCBb. 1%DMGSs associated with CCBbs occurred over the whole UK apart from the southern coast of England. 1%DMGSs associated with the WCB also occurred over all parts of the country, which is unsurprising given the typically large area of the WCB relative to some of the other identified features [*Hewson and Neu*, 2015] (Table 1). The CCB (a and b combined) and WCB account for far fewer 0.1%DMGSs, showing that while causing widespread strong winds, they are not so often associated with the most severely damaging (top 0.1%) winds.

Table 2. The 2008–2014 Subsynoptic-Scale Features[a]

Gust Causing Mechanism	Total 1%DMGS (%)	Total 0.1%DMGS (%)	Percentage of 1%DMGSs Also 0.1%DMGSs
Returning cold conveyor belt (CCBb)	205 (34.2%)	9 (22%)	4.4%
Warm conveyor belt (WCB)	100 (16.7%)	4 (9.8%)	4%
Convective line (CL)	78 (13%)	10 (24.4%)	12.8%
Pseudo-CL	74 (12.3%)	6 (14.7%)	8.1%
Cold conveyor belt (CCBa)	31 (5.2%)	1 (2.4%)	3.2%
Dry conveyor belt (DCB)	30 (5%)	1 (2.4%)	3.3%
Convective systems (CS) and dry slot convective systems	23 (3.8%)	0	0
Potential sting jet (SJ)	21 (3.5%)	10 (24.4%)	47.6%
Unclassified	38 (6.3%)	0	0
Total	600	41	

[a]The 2008–2014 subsynoptic-scale features associated with the top 1% and 0.1% of DMGSs. Note that thresholds are based on the full 1980–2014 data set; hence, the proportion of 1%DMGS to 0.1%DMGS is not 10%.

Table 2 demonstrates the importance of CLs in the production of damaging winds in the UK. *Clark* [2013] showed that CLs occur frequently in the UK during the autumn and winter months, and the results here indicate that they are also very influential in causing some of the most extreme UK surface winds, accounting for over 13% of 2008–2014 1%DMGS and almost a quarter of all 0.1%DMGSs. The spatial distribution of CLs (not shown) has them mostly located in the southern half of the UK, in accordance with *Clark* [2013], CLs often dissipating on encountering the mountainous topography of the interior of northern Britain. An exception to this occurred, however, during windstorm Xaver where 9 of the 11 1%DMGSs in northern Britain were attributed to these features occurring as two organized bands of heavy precipitation passing over the area, associated with primary and secondary cold fronts. Six of these were 0.1%DMGSs, showing that these systems can cause highly damaging winds anywhere in the UK.

Pseudo-CLs (Table 1) were associated with just over 12% of the 1%DMGS and 15% of 0.1%DMGSs, including fronts, troughs, and pre-/post-CL (not shown) situations during windstorms. These occurred during the "cool season" (September–February) and were not large enough spatially, long enough temporally, or intense enough to feature in *Clark*'s [2013] CL climatology. However, they still produced extreme surface wind speeds, indicating that the *Clark* [2013] CL threshold criteria (Table S1), designed primarily to identify the more extensive and intense examples of narrow cold frontal rainbands, may be too rigid for directly repurposing to UK extreme wind gust applications. The latter is further supported by the geographical distribution of pseudo-CLs here being less weighted toward the south of the UK, implying that 2008–2014 CLs in the north were generally less strong, less long lived, and less extensive. However, CL frequencies in *Clark*'s [2013] 2003–2010 climatology were nonzero over most of the north of the UK, so CLs are not completely unknown in this region as exemplified by windstorm Xaver. CLs and pseudo-CLs (when combined) are very important contributors to UK extreme winds, accounting for over a quarter of 1%DMGSs and more than a third of 0.1%DMGSs, making them the most important ETC mechanism for producing extreme surface winds.

During the 2008–2014 period, there were at least three known SJ-producing ETCs identified in the literature, Friedhelm on 8 December 2011 [*Baker et al*., 2013; *Martínez-Alvarado et al*., 2014; *Vaughan et al*., 2015], Ulli on 3 January 2012 [*Smart and Browning*, 2014], and Christian on 28 October 2013 [*Browning et al*., 2015]. SJs were also allocated as the cause of 0.1%DMGSs during each of these events during our study. Twenty one of the 600 1%DMGS were diagnosed as potentially being caused by SJs. Over 10 ETCs were originally considered as potential including SJs based on the location of the gust, and cloud head, but were subsequently shown to have an insufficient central pressure deepening rate [*Browning*, 2004] and/or there was no obvious evidence of cloud banding in satellite images (not shown). So the closely located CCBb is the feature most likely associated with these gusts. It has not been possible here to effectively distinguish between SJs and the CCBb during frontal "T-bone" development (stage III and between III and IV) using the observational and relatively coarse model output tools available (ERA-interim); hence, these 21 1%DMGS remain "potential" SJs [see *Martínez-Alvarado et al*., 2014]. These events are an important set. Of the 21 1%DMGSs, 10 (47.6%) are also 0.1%DMGSs, showing how extreme they can be, making up almost a quarter of all 0.1%DMGSs. This continues the pattern, along with CLs, of smaller-scale features producing the most damaging (top 0.1%) gusts.

A northern and western UK spatial distribution of potential SJs is seen in our study, with the exception of windstorm Christian which produced potential SJs over the south of England at seven different sites (Figure S2). A possible reason for this is that SJs occur midway through an ETCs life cycle, during or just after the rapid deepening of ETCs that form in the genesis region in the relatively warm waters of the eastern Atlantic; ETCs are more likely to form and develop over the sea than over land [*Dacre and Gray*, 2009]. This implies less rapid deepening and therefore less SJ potential over eastern UK locations, eastward tracking ETCs losing their energy source once they reach land. However, when they do reach this region, they have a major impact. *Browning* [2004] found that for the October 1987 storm, a SJ formed in eastern England, though the exceptional SW-NE orientation of this track may have added to the low-level convectional forcing of this ETC from the relatively warm English Channel. This meant that the ETC was still intensifying when it reached the south coast of England, unlike the majority of east Atlantic forming storms that have a more W-E track [*Dacre and Gray*, 2009]. This is similar to the track observed during windstorm Christian. We are not aware of a previous study of the geographical spread of surface SJs as we highlight in Figure S2; *Martínez-Alvarado et al.* [2012] did highlight the SJ precursor areas in relation to the ETC center, indicating that tracks of such cyclones tended to begin farther south than the general average. All other SJ-related publications are case study based. *Hewson and Neu* [2015] indicate the position of SJs in relation to the storm track, though this is not based on surface observations.

The 0.1%DMGS results highlight the importance of some subsynoptic-scale features which are perhaps not always given the attention that their surface impacts merit. There is currently much concentration in the literature on the formation of SJs responsible for extreme gusts within ETCs [*Browning*, 2004; *Clark et al.*, 2005; *Martínez-Alvarado et al.*, 2012; *Smart and Browning*, 2014; *Browning et al.*, 2015]. Our results suggest that greater focus could also be usefully paid to CL/pseudo-CL features which, based on the station network utilized here, are associated with a third of the most damaging observed UK surface gusts during the 2008–2014 period.

4. Conclusions

The main objective of this paper was to construct a 2008–2014 climatology of UK ETC subsynoptic-scale features associated with the highest surface wind gusts recorded across a network of UK surface stations. A novel way to quantify the relative contributions of mesoscale ETC features was introduced. We demonstrate that larger-scale features (WCB and CCB) dominate the top 1% of UK extreme winds; however, it is the smaller-scale mechanisms, CLs and SJs, which produce the most intense (top 0.1%) gusts. The CCB is split into two categories, ahead of the warm front (CCBa) and when returning from the poleward side of the low-pressure center (CCBb). The CCB is most hazardous when joining the direction of ETC travel, during CCBb, accounting for 34% of 1%DMGSs and 22% of 0.1%DMGSs, whereas the CCBa accounts for 5% and 2%, respectively. CLs and pseudo-CLs account for 13% and 12%, respectively, of the top 1% of DMGSs and also greatly influence the top 0.1% (24% and 15%, respectively); convective lines merit more attention. Potential SJs account for 3.5% of 1%DMGSs, but these events are particularly significant, almost half also being categorized as 0.1%DMGSs, accounting for 24% of the strongest winds seen at UK observation stations in this period despite their small-scale nature.

Going forward, we plan to extend this 2008–2014 climatology into the future. A recent study by *Schemm et al.* [2016] has indicated that extremely active fronts are becoming more frequent over Europe, especially since the year 2000, so this work will become crucial in our understanding of the UK wind regime in a changing climate. After first lengthening our climatology, we also plan to conduct seasonal analysis on each of the individual ETC features responsible for the most damaging UK gusts.

Acknowledgments
This research was kindly funded by the Worshipful Company of Insurers and the Australian Research Council grant DP16010997. Our thanks go to the UK Met Office for providing the wind speed and radar data via the British Atmospheric Data Centre (BADC; available at http://badc.nerc.ac.uk/data/ukmo-midas/ukmo_guide.html). We would also like to acknowledge the University of Dundee Satellite Receiving Station (available at http://www.sat.dundee.ac.uk/) for access to satellite imagery and Richard Hewston for his part in the creation of the DMGS database. Our thanks goes to Matthew Clark, who provided useful feedback on the "convective lines" part of the project. We would also like to acknowledge the contribution of the late Roland von Glasow, who was highly influential in the early discussions of this work, providing exceptional insight and knowledge.

References

Baker, L. (2009), Sting jets in severe northern European wind storms, *Weather*, *64*(6), 143–148.
Baker, L., O. Martinez-Alvarado, J. Methven, and P. Knippertz (2013), Flying through extratropical cyclone Friedhelm, *Weather*, *68*(1), 9–13.
Bjerknes, J., and H. Solberg (1922), Life cycle of cyclones and the polar front theory of atmospheric circulation, *Geophys. Publ.*, *3*, 1–18.
Brönnimann, S., O. Martius, H. von Waldow, C. Welker, J. Luterbacher, G. P. Compo, P. D. Sardeshmukh, and T. Usbeck (2012), Extreme winds at northern mid-latitudes since 1871, *Meteorol. Z.*, *21*(1), 13–27.
Browning, K. A. (1990), Organization of clouds and precipitation in extratropical cyclones, in *Extratropical Cyclones: The Erik Palmen Memorial Volume*, edited by C. W. Newton and E. O. Holopainen, pp. 129–153, Am. Meteorol. Soc., Boston, Mass.

Browning, K. A. (2004), The sting at the end of the tail: Damaging winds associated with extratropical cyclones, *Q. J. R. Meteorol. Soc.*, *130*(597), 375–399.
Browning, K. A., D. J. Smart, M. R. Clark, and A. J. Illingworth (2015), The role of evaporating showers in the transfer of sting-jet momentum to the surface, *Q. J. R. Meteorol. Soc.*, *141*(693), 2956–2971.
Carlson, T. N. (1980), Airflow through midlatitude cyclones and the comma cloud pattern, *Mon. Weather Rev.*, *108*, 1498–1509.
Clark, M. R. (2013), A provisional climatology of cool-season convective lines in the UK, *Atmos. Res.*, *123*, 180–196.
Clark, P. A., K. A. Browning, and C. Wang (2005), The sting at the end of the tail: Model diagnostics of fine-scale three-dimensional structure of the cloud head, *Q. J. R. Meteorol. Soc.*, *131*(610), 2263–2292.
Cotton, W. R., and R. A. Anthes (1989), *Storm and Cloud Dynamics*, *Int. Geophys. Series*, vol. 44, p. 883, Academic Press.
Dacre, H. F., and S. L. Gray (2009), The spatial distribution and evolution characteristics of North Atlantic cyclones, *Mon. Weather Rev.*, *137*, 99–115.
Dacre, H. F., M. K. Hawcroft, M. A. Stringer, and K. I. Hodges (2012), An extratropical cyclone atlas: A tool for illustrating cyclone structure and evolution characteristics, *Bull. Am. Meteorol. Soc.*, *93*(10), 1497–1502.
Davis, C., et al. (2004), The bow Echo and MCV experiment, *Bull. Am. Meteorol. Soc.*, *85*, 1075–1093.
Earl, N. (2013), The UK wind regime-observational trends and extreme event analysis and modelling, PhD thesis, Univ. of East Anglia.
Earl, N., S. Dorling, R. Hewston, and R. von Glasow (2013), 1980–2010 variability in UK surface wind climate, *J. Clim.*, *26*, 1172–1191, doi:10.1175/JCLI-D-12-00026.1.
Gatzen, C., T. Púčik, and D. Ryva (2011), Two cold-season derechoes in Europe, *Atmos. Res.*, *100*(4), 740–748.
Gray, S. L., O. Martínez-Alvarado, L. H. Baker, and P. A. Clark (2011), Conditional symmetric instability in sting-jet storms, *Q. J. R. Meteorol. Soc.*, *137*(659), 1482–1500.
Hanna, E., T. E. Cropper, P. D. Jones, A. A. Scaife, and R. Allan (2015), Recent seasonal asymmetric changes in the NAO (a marked summer decline and increased winter variability) and associated changes in the AO and Greenland blocking index, *Int. J. Climatol.*, *35*(9), 2540–2554.
Hewson, T. D., and U. Neu (2015), Cyclones, windstorms and the IMILAST project, *Tellus A*, *67*, 27128.
Hewston, R. (2008), Weather, climate and the insurance sector, PhD thesis, Univ. of East Anglia.
Hewston, R., and S. R. Dorling (2011), An analysis of observed maximum wind gusts in the UK, *J. Wind. Eng. Ind. Aerod.*, *99*, 845–856, doi:10.1016/j.jweia.2011.06.004.
Lamb, H. H. (1950), Types and spells of weather around the year in the British isles: Annual trends, seasonal structure of the year, singularities, *Quart. J. Royal Met. Soc.*, *76*(330), 393–438.
Martínez-Alvarado, O., S. L. Gray, J. L. Catto, and P. A. Clark (2012), Sting jets in intense winter North-Atlantic windstorms, *Environ. Res. Lett.*, *7*, 024014.
Martínez-Alvarado, O., L. H. Baker, S. L. Gray, J. Methven, and R. S. Plant (2014), Distinguishing the cold conveyor belt and sting jet airstreams in an intense extratropical cyclone, *Mon. Weather Rev.*, *142*(8), 2571–2595.
Neu, U., et al. (2013), IMILAST: A community effort to intercompare extratropical cyclone detection and tracking algorithms, *Bull. Am. Meteorol. Soc.*, *94*(4), 529–547.
Parton, G. A., G. Vaughan, E. G. Norton, K. A. Browning, and P. A. Clark (2009), Wind profiler observations of a sting jet, *Q. J. R. Meteorol. Soc.*, *135*(640), 663–680.
Parton, G., A. A. Dore, and G. Vaughan (2010), A climatology of midtropospheric mesoscale strong wind events as observed by the MST radar, Aberystwyth, *Meteor. Appl.*, *17*, 340–354, doi:10.1002/met.203.
Schemm, S., M. Sprenger, O. Martius, H. Wernli, and M. Zimmer (2016), Increase in the number of extremely strong fronts over Europe?—A study based on ERA-Interim reanalysis (1979–2014), *Geophys. Res. Lett.*, *44*, 553–561, doi:10.1002/2016GL071451.
Schultz, D. M. (2001), Reexamining the cold conveyor belt, *Mon. Weather Rev.*, *129*, 2205–2225.
Schultz, D. M., and G. Vaughan (2011), Occluded fronts and the occlusion process: A fresh look at conventional wisdom, *Bull. Am. Meteorol. Soc.*, *92*(443–466), ES19–ES20.
Schultz, D. M., D. Keyser, and L. F. Bosart (1998), The effect of largescale flow on low-level frontal structure and evolution in midlatitude cyclones, *Mon. Weather Rev.*, *126*, 1767–1791.
Shapiro, M. A., and D. Keyser (1990), Fronts, jet streams and the tropopause. Extratropical cyclones, the Erik Palmen memorial volume, edited by C. W. Newton and E. O. Holopainen, pp. 167–191, Am. Meteorol. Soc., Boston, Mass.
Smart, D. J., and K. A. Browning (2014), Attribution of strong winds to a cold conveyor belt and sting jet, *Q. J. R. Meteorol. Soc.*, *140*(679), 595–610.
Swiss Re (2016), Natural catastrophes and man-made disasters in 2015: Historic losses surface from record earthquakes and floods, sigma, no 1/2016.
Tilinina, N., S. K. Gulev, I. Rudeva, and P. Koltermann (2013), Comparing cyclone life cycle characteristics and their interannual variability in different reanalyses, *J. Clim.*, *26*(17), 6419–6438.
Vaughan, G., et al. (2015), Cloud banding and winds in intense European cyclones: Results from the DIAMET project, *Bull. Am. Meteorol. Soc.*, *96*(2), 249–265.
Vautard, R., J. Cattiaux, P. Yiou, J. Thépaut, and P. Ciais (2010), Northern hemisphere atmospheric stilling partly attributed to an increase in surface roughness, *Nat. Geosci.*, *3*, 756–761, doi:10.1038/NGE0979.
Wang, X. I., F. W. Zwiers, V. R. Swail, and Y. Feng (2009), Trends and variability of storminess in the Northeast Atlantic region, 1874–2007, *Clim. Dyn.*, *33*, 1179–1195.
Weisman, M. L. (2001), Bow echoes: A tribute to TT Fujita, *Bull. Am. Meteorol. Soc.*, *82*(1), 97–116.
Wheatley, D. M., R. J. Trapp, and N. T. Atkins (2006), Radar and damage analysis of severe bow echoes observed during BAMEX, *Mon. Weather Rev.*, *134*(3), 791–806.
Woodroffe, A. (1988), Summary of weather pattern developments of the storm of 15/16 October 1987, *Meteor. Mag.*, *117*, 99–103.